Cell Death and Differentiation (2012) 19, 1590–1601

www.nature.com/cdd

Autophagy and phagocytosis-like cell cannibalism exert opposing effects on cellular survival during metabolic stress

J Poels[1,2,3,6], MR Spasić[1,4,6], M Gistelinck[1,2,3], J Mutert[1,2,4], A Schellens[1,2,3], P Callaerts[1,2,3] and KK Norga*[,1,4,5]

Understanding mechanisms controlling neuronal cell death and survival under conditions of altered energy supply (e.g., during stroke) is fundamentally important for the development of therapeutic strategies. The function of autophagy herein is unclear, as both its beneficial and detrimental roles have been described. We previously demonstrated that loss of AMP-activated protein kinase (AMPK), an evolutionarily conserved enzyme that maintains cellular energy balance, leads to activity-dependent degeneration in neuronal tissue. Here, we show that energy depletion in *Drosophila* AMPK mutants results in increased autophagy that convincingly promotes, rather than rescues, neurodegeneration. The generated excessive autophagic response is accompanied by increased TOR and S6K activity in the absence of an AMPK-mediated negative regulatory feedback loop. Moreover, energy-depleted neurons use a phagocytic-like process as a means to cellular survival at the expense of surrounding cells. Consequently, phagocytosis stimulation by expression of the scavenger receptor Croquemort significantly delays neurodegeneration. This study thus reveals a potentially novel strategy for cellular survival during conditions of extreme energy depletion, resembling xeno-cannibalistic events seen in metastatic tumors. We provide new insights into the roles of autophagy and phagocytosis in the neuronal metabolic stress response and open new avenues into understanding of human disease and development of therapeutic strategies.
Cell Death and Differentiation (2012) **19**, 1590–1601; doi:10.1038/cdd.2012.37; published online 13 April 2012

Cells survive and adapt to periods of energetic stress (e.g., during starvation) by induction of compensatory processes that ensure the continuation of energy supply, major of which is autophagy. Macroautophagy (herein referred to as autophagy) is an evolutionarily conserved catabolic process in which intracellular macromolecules and complete organelles are sequestered in double-membrane vesicles (autophagosomes) and delivered to the lysosome (by fusion and formation of autolysosomes) for degradation. Subsequently, the resulting breakdown products are recycled back to the cytoplasm providing inputs to cellular metabolism. Autophagy is linked to the cellular metabolic status via its negative regulator, target of rapamycin (TOR), and its upstream kinase, AMP-activated protein kinase (AMPK).[1] AMPK is an evolutionarily conserved serine/threonine kinase that senses changes in energy levels through AMP, and adapts cellular metabolism by regulating an array of catabolic and anabolic processes.[2] Composed of three subunits (α, β and γ, each of which is essential for its catalytic activity), AMPK stimulates autophagy by inhibition of TOR, but also by directly phosphorylating ULK1 (mammalian homolog of yeast and fly Atg1, a kinase essential for autophagy initiation).[3,4] However, other AMPK-independent (as well as TOR-independent) routes of autophagy stimulation exist.[5]

Despite having an important role in starvation and stress responses, the role of autophagy in cellular death and survival is controversial.[6] Although it remains clear that autophagy promotes cellular survival in multiple physiological and experimental settings, by executing clearance of misfolded proteins, old or damaged cellular components (and thus also preventing degenerative diseases), autophagic hallmarks have often been observed in dying cells and have been associated with type II programmed cell death.[7] In addition, in *Drosophila* larval salivary glands and midgut, autophagy-mediated cellular degradation is induced as part of the normal developmental process.[8,9] Recently, several cell engulfment receptors were identified as essential for complete autophagic destruction of *Drosophila* salivary glands, while dispensable for starvation-induced autophagy.[10] Finally, while direct

[1]Laboratory of Behavioral and Developmental Genetics, Leuven 3000, Belgium; [2]VIB Center for the Biology of Disease, Leuven 3000, Belgium; [3]Department of Human Genetics, KU Leuven, Leuven 3000, Belgium; [4]Department of Woman and Child, KU Leuven, Leuven 3000, Belgium and [5]Department of Pediatric Oncology, Antwerp University Hospital, Edegem 2650, Belgium
*Corresponding author: KK Norga, Laboratory of Behavioral and Developmental Genetics, KU Leuven and Pediatric Oncology, Antwerp University Hospital, 10 Wilrijkstraat, Edegem B-2650, Belgium. Tel: +32 3 8213182; Fax: +32 3 8291194; E-mail: Koen.Norga@uza.be
[6]These authors contributed equally to this work.
Keywords: AMPK; autophagy; *Drosophila*; metabolism; neurodegeneration; phagocytosis
Abbreviations: alc, alicorn; AMPK, AMP-activated protein kinase; Crq, Croquemort; DIAP, *Drosophila* inhibitor of apoptosis; Drpr, draper; EGUF, eyeless-Gal4 UAS-Flippase; ERG, electroretinogram; ey, eyeless; GMR-hid, glass multimer reporter-head involution defective; LC3, microtubule-associated protein 1 light chain 3; MARCM, mosaic analysis with a repressible cell marker; Shi, shibire; TOR, target of rapamycin; TSC, tuberous sclerosis complex; UAS, upstream activator sequence; ULK, Unc-51-like kinase
Received 09.9.11; revised 02.3.12; accepted 02.3.12; Edited by S Kumar; published online 13.4.12

induction of autophagy by overexpression of Atg1 induces apoptotic cell death in *Drosophila*,[11] only a handful of studies have yet demonstrated that knockdown/knockout of *atg* (*autophagy*) genes reduces cell death.[12] Therefore, molecular mechanisms and metabolic contexts determining decisions between autophagy-mediated cellular survival and autophagy-associated cell death remain poorly understood.

To approach these questions, we used a model of energy depletion as it occurs in AMPK-deficient neuronal tissue of *Drosophila*. We previously showed that removal of β-AMPK in the visual system of the fruitfly results in progressive neurodegeneration, arising as a consequence of neuronal activity (and subsequent energy depletion). This progressive phenotype is characterized by increasing vacuolization and loss of photoreceptors in the retina and is accompanied by behavioral defects that increase in severity with aging.[13] Here, we demonstrate that in these metabolic conditions, autophagy is strongly upregulated, promoting neurodegeneration. Moreover, lack of AMPK activity is accompanied by increased TOR activity and, importantly, the absence of negative regulatory feedback from autophagy toward AMPK. In normal conditions this potentially serves to limit excessive activation of the autophagic response. Finally, we provide evidence that photoreceptor neurons compensate energy depletion by a form of phagocytic cannibalism of surrounding cells, which can be stimulated with expression of the scavenger receptor Croquemort (Crq). In this report, we thus present new insights on how cells adapt to and survive periods of severe metabolic perturbation.

Results

β-AMPK deficiency leads to non-apoptotic neurodegeneration. β-AMPK (termed *alicorn* or *alc*) deficiency in the *Drosophila* eye leads to progressive retinal degeneration, characterized by extensive vacuolization, the presence of large vesicular structures, loss of photoreceptor neurons and general structural disorganization (Figure 1a). This is almost completely prevented by genetically or functionally inhibiting the activity of photoreceptor neurons, and thus is a consequence of their activity and resulting energy depletion.[13] In order to determine the cause of cellular degeneration, we first investigated the involvement of caspase-dependent apoptosis. To this end, we tested whether p35 and DIAP1 (a baculoviral and a *Drosophila* caspase inhibitor, respectively) could rescue the neurodegenerative phenotype of β-AMPK mutants. Neither p35 nor DIAP1 suppressed the *alc* retinal phenotype, indicating that the observed neuronal degeneration is not caused by caspase-dependent apoptosis (Spasić *et al.*[13] and Figure 1a).

To more closely investigate the morphology of dying cells, we performed transmission electron microscopy on mutant retinas. None of the typical hallmarks of apoptosis (chromatin condensation, nuclear fragmentation, plasma membrane blebbing and cell shrinkage) could be discerned not at early stages (day 1, data not shown), nor at very late stages of degeneration (day 14, Figure 1b), supporting the conclusion that this degenerative process is non-apoptotic.

Autophagy promotes neurodegeneration in *alc* mutants. The detailed analysis of the electron micrographs revealed expansion of the lysosomal compartment, a number of multilamellar inclusions, multivesicular endosomes, as well as vesicles that likely correspond to autophagosomes with partially degraded cytoplasmic material (Figures 1b and c). These features were particularly prominent in later stages of degeneration, and being typical hallmarks of autophagy, suggested an upregulation of this process. In support of this conclusion, in degenerating mutant brains we found a marked appearance of punctate localization of GFP-LC3 (microtubule-associated protein 1-light chain 3, the mammalian ortholog of yeast and fly Atg8), a commonly used marker for autophagosomes and autolysosomes.[14] In addition, functional inactivation of these neurons (many of which relay information from photoreceptors), achieved by rearing flies in the dark, completely suppressed the punctate staining pattern (Figure 2a), demonstrating that formation of GFP-LC3 punctae and thus autophagy upregulation was a consequence of energy deprivation in an AMPK-deficient background, and not just the mere absence of AMPK. Finally, using LysoTracker to label acidic cellular compartments (such as the (auto)lysosomes), we showed that GFP-LC3-positive punctae co-localize with LysoTracker-positive spots in immunostainings, conclusively demonstrating the presence of autolysosomes in *alc* mutant flies (Figure 2a). Consistent with this, we also observed normal induction of autophagy in the larval fat body of *alc* mutants (Supplementary Figure S1). These results were unexpected, given that AMPK, which is absent in *alc* mutants, is a major stimulator of autophagy.

We next determined whether autophagy induction is (partly) responsible for neurodegeneration of *alc* mutants. To this end, we downregulated autophagy in mutant tissues using loss-of-function alleles of *Atg8a* (*Atg8a*^{KG07569}) and *Atg7* (*Atg7*^{d4}), or a dominant-negative (kinase-defective) form of *Atg1* (*Atg1*^{K38Q}). In the *Atg8a* mutant background or after *Atg1*^{K38Q} overexpression, *alc* mutants showed a strong improvement in retinal morphology: photoreceptor loss was almost entirely absent and ommatidial organization was largely preserved (Figures 2b and c). For subsequent functional analysis, flies were subjected to electroretinogram (ERG) recordings that measure the collective response of retinal cells to a light stimulus. Compared with heterozygous controls, *alc* mutants are characterized by a marked reduction of both 'on-' and 'off-transients' (indicating synaptic activity of photoreceptors) and LCRP (light coincident receptor potential, resulting from depolarization of photoreceptors in response to a light stimulus). These defects were significantly reverted in an *Atg7* mutant background at day 1, and remained substantially improved at day 7 (Figure 2d and Supplementary Figure S2).

In conclusion, both ultrastructural analysis and appearance of autophagosome and autolysosome markers meet the criteria for autophagic cell death as recently defined and thus demonstrate an upregulated autophagic response in degenerating *alc* mutant tissues.[6] Importantly, the degenerative morphological and functional defects can be rescued by downregulation of autophagy.

Detrimental effects of autophagy are restricted to *alc* mutants. To investigate if the detrimental effects of autophagy are a consequence of general excessive stimulation of

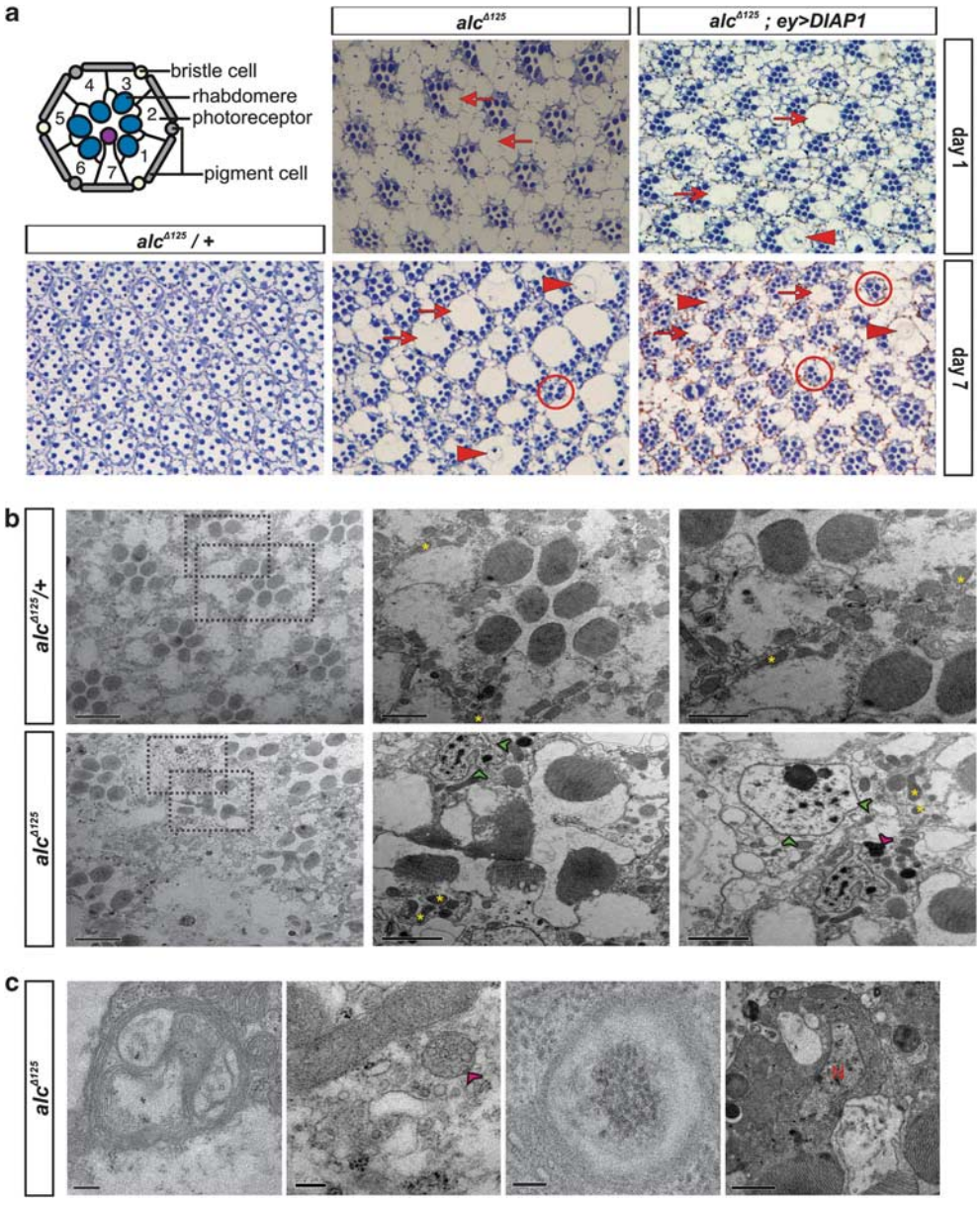

Figure 1 Neuronal death in β-AMPK (*alc*) mutants is not caused by caspase activation. (**a**) The *Drosophila* compound eye is a regular array of $\sim$800 units (ommatidia) each consisting of 8 photoreceptor neurons and 12 accessory cells. On tangential sections (which are represented here) seven photoreceptors are visible, and can be discerned by their apical membrane domains specialized in light perception (rhabdomeres; represented as dark-stained spots in light micrographs). Overexpression of caspase inhibitors p35[13] or DIAP1 does not rescue the *alc*-associated retinal degeneration in 1- or 7-day-old *alc* mutants. Representative examples of vacuolization (arrows), vesicular structures (arrowheads) and rhabdomere loss (circles) are indicated. As a control, a 7-day-old heterozygous *alc* eye section is depicted. Overexpression of DIAP1 alone does not lead to retinal degeneration (not shown). $alc^{\Delta 125}$, null allele of β-*AMPK* (*alc*); *ey*, *eyeless*-mediated overexpression. Diagram of ommatidial cross-section adapted from Wang and Montell.[41] (**b**) Ultrastructural analysis of 14-day-old *alc* mutant tissues by transmission electron microscopy reveals no typical hallmarks of apoptosis (such as chromatin condensation, nuclear fragmentation, plasma membrane blebbing and cell shrinkage). Compared with heterozygous controls (top row of panels), ommatidial architecture in *alc* mutants (bottom row) is highly disorganized, with clear signs of cellular degeneration: vacuolization and abundant vesicular structures, some of which are very large (green arrowheads) and appear to contain degraded cellular material. Some vesicles contain multilamellar inclusions (magenta arrowhead). Representative mitochondria are indicated with a yellow asterisk. Scale bars; 5 μm (panels on far left) and 2 μm (magnifications of boxed areas, panels on the right). (**c**) Autophagic hallmarks, such as multilamellar inclusions (left panel), multivesicular endosomes (second panel, magenta arrowhead) and double-membrane bound electron-dense cellular material (third panel) are frequently observed in 14-day-old mutant tissues. A representative nucleus (N) of an *alc* mutant photoreceptor is shown in the right panel. Scale bars; 200 nm (left and second panel), 100 nm (third panel) and 2 μm (right panel). Genotypes: *FRT42D,*$alc^{\Delta 125}$*/+ ; EGUF/+* ($alc^{\Delta 125}$*/+* panels), *FRT42D,*$alc^{\Delta 125}$*/FRT42D,GMR-hid,l(2)CI-R1; EGUF/+* ($alc^{\Delta 125}$ panels) and *FRT42D,*$alc^{\Delta 125}$*/FRT42D,GMR-hid,l(2)CI-R1; EGUF/UAS-DIAP1*

this process, or are specific for severe metabolic depletion occurring in *alc* mutants, we stimulated the autophagic response in both wild-type and *alc* mutant animals. We achieved this by treating the flies with 2 μM rapamycin, which induces autophagy by inhibiting TOR (a negative regulator of autophagy), or 5 mM LiCl, which enhances autophagy

independently of TOR, by inhibiting inositol monophosphatase. None of these treatments resulted in retinal degeneration in wild-type flies or in a rescue from neurodegeneration in *alc* mutants (Figure 3a). We further investigated whether upregulation of autophagy resulted in aggravation of neurodegeneration in *alc* mutants. The extent of degeneration is smaller in dark-reared *alc* mutant flies when compared with flies reared on a light/dark cycle,[13] thus providing a more sensitive background for investigation of additive effects. Upregulation of *Atg8a*, a rate-limiting autophagy gene, which promotes the autophagic response clearly resulted in aggravation of neurodegeneration in *alc* mutants (Figure 3b). These results strongly suggest that autophagy is not detrimental for cellular survival *per se*, but does have a significant role in the pathology of *alc* mutants.

***alc* mutants display increased TOR activity.** To investigate the mechanism by which autophagy is upregulated in the absence of AMPK, we first examined the function of TOR. TOR kinase is inhibited by AMPK either directly or indirectly, while chronic activation of TOR leads to increased AMPK activity, providing a negative regulatory feedback loop.[15] Therefore, the absence of AMPK would lead to increased TOR activity. Indeed, western blots of *alc* head extracts labeled with a phospho-specific antibody against *Drosophila* p70 S6 kinase (dS6K, a well-known TOR substrate of which the phosphorylation status is frequently used as a measure for TOR activity[15]) revealed a significant increase in dS6K phosphorylation and thus TOR activity in *alc* mutants when compared with heterozygous controls (Figure 4a). Although activation of TOR would result in suppression of the autophagic response, at the same time dS6K promotes rather than suppresses autophagy,[16] and its increased activity in *alc* mutants could at least partially account for the observed enhancement of autophagy. However, other, TOR-unrelated mechanisms of autophagy upregulation in β-AMPK mutants most likely contribute.

In agreement with these conclusions, inhibition of TOR in *alc* mutants by overexpression of dTSC2, or a TOR domain that serves as a dominant-negative allele ($dTOR^{FRB}$), not only did not improve the degenerative phenotype, but instead resulted in its aggravation (shown for 7-day-old flies, Figure 4b), most likely as a result of further increases in autophagic activity. Similar results were obtained after overexpression of a constitutively active dS6K ($dS6K^{STDE}$; Figure 4b). These data further support the deleterious effects of autophagy in the context of AMPK deficiency.

Increased autophagy partially results from the lack of negative feedback regulation of AMPK. To closer examine the relationship between autophagy and AMPK activity, we induced autophagy by ubiquitous overexpression of Atg8a in wild-type flies, and measured AMPK activation by monitoring the phosphorylation status of Thr184 in the catalytic α-subunit of *Drosophila* AMPK (corresponding to Thr172 in human AMPK-α2). Phosphorylation of Thr184 (therefore AMPK activation) was severely reduced in Atg8a-overexpressing flies when compared with the controls (Figure 4c). Similar results were obtained upon autophagy upregulation by rearing flies on food supplemented with 5 mM LiCl (data not shown). This strongly suggests that an increased autophagic response negatively regulates AMPK activity in a regulatory feedback loop, thereby limiting its levels in conditions of persistent activation. The absence of this negative regulation in *alc* mutants most likely significantly contributes to the excessive induction of autophagy.

Loss of AMPK reveals a phagocytosis-like neuronal survival mechanism in early stage degeneration. During detailed ultrastructural analysis of early stage (day 1) degenerating retinal tissue of *alc* mutants, we noticed further peculiarities. Namely, in contrast to photoreceptor neurons whose cellular content was very rich in mitochondria, granulated or 'rough' endoplasmic reticulum and other organelles, the pigment cells that surround them appeared to mostly contain large vesicular structures with degraded cellular content (Figure 5a). Moreover, photoreceptors seemed to display an internalization process at the cell surface, where very large vesicles (often exceeding 500 nm in diameter) filled with electron-dense material were frequently observed (Figure 5b). On the basis of the size of the engulfed particles, which was beyond the limit for most major endocytic routes except phagocytosis,[17] we concluded that photoreceptors exert a phagocytic-like activity.

As phagocytosis presents a potential mechanism for energy acquisition,[18] we hypothesized that this could be compensatory behavior of photoreceptor neurons in early stages of energy deprivation, complementary to autophagy, and that downregulation of this process would worsen the neurodegeneration in *alc* mutants. As a first approach to influence phagocytosis, we overexpressed a dominant-negative allele of *shibire* (shi^{K44A}) in the *alc* mutant background. Shibire is the fly ortholog of vertebrate dynamin, a GTPase that is necessary for certain types of endocytosis, as well as for phagocytosis.[19] Downregulation of shibire caused a marked aggravation of *alc*-mediated neurodegeneration at day 1, as well as at day 7. This experiment was carried out in the dark, with photoreceptors mostly inactive, thereby ruling out a major influence of the shibire mutation on photoreceptor neurotransmission or on the formation of autophagosomes. In order to more specifically target phagocytosis, we downregulated Draper, the *Drosophila* ortholog of the *Caenorhabditis elegans* engulfment receptor CED-1.[20] Draper is involved in glia-mediated engulfment of cell corpses and downregulation of Draper aggravated *alc*-mediated neurodegeneration (Figure 5c). We next tested if stimulation of phagocytic-like activity ameliorates the degeneration of *alc* mutant flies. Crq is a CD36-related scavenger receptor involved in the clearance of apoptotic cells during *Drosophila* embryogenesis. Exogenous Crq expression in COS cells or neurons confers the ability to phagocytose cells undergoing apoptosis.[21,22] The overexpression of Crq in mutant *alc* eyes significantly delayed retinal degeneration (Figure 5d), strongly suggesting that photoreceptor neurons use phagocytic ability as means of survival in metabolic perturbation conditions. Interestingly, Crq overexpression in homozygous *alc* flies also reverted the phosphorylation status of dS6K to the level of heterozygous *alc* control flies (Supplementary Figure S3).

Discussion

Neurons are especially sensitive to cellular energy fluctuations because of their high metabolic demands and low capacity to store nutrients. This is particularly acute in the retina that possesses one of the highest metabolic rates of all tissues in the body. We used the activity-dependent cellular metabolic perturbation that occurs in AMPK-deficient *Drosophila* retina as a model to study adaptive responses of neurons to metabolic stress.

Basal levels of autophagy are necessary in all cells, and serve homeostatic functions, such as cytoplasmic protein and organelle turnover. The autophagic response is rapidly upregulated with increased cellular energy demands, which cannot be met by the nutrient supply (e.g., during starvation). In that respect autophagy serves a similar purpose to AMPK activation under these conditions; that is to restore cellular energy levels. Therefore, it is not surprising that regulation of the two pathways, the autophagic response and AMPK pathway, is interconnected. In addition to AMPK, several other molecules regulate autophagy via TOR-dependent or -independent routes, for example, deacetylase Sirt1, Ras GTPase, FOXO transcription factor and several kinases, some acting in the absence of AMPK.[23,24]

In our study, we find no morphological or genetic evidence for involvement of apoptosis in neurodegeneration of β-AMPK (*alc*) mutants, in agreement with an earlier study in which TUNEL staining of γ-AMPK degenerating brains was negative.[25] Instead, we observe a severe upregulation of autophagy, which promotes neurodegeneration in an *alc* mutant

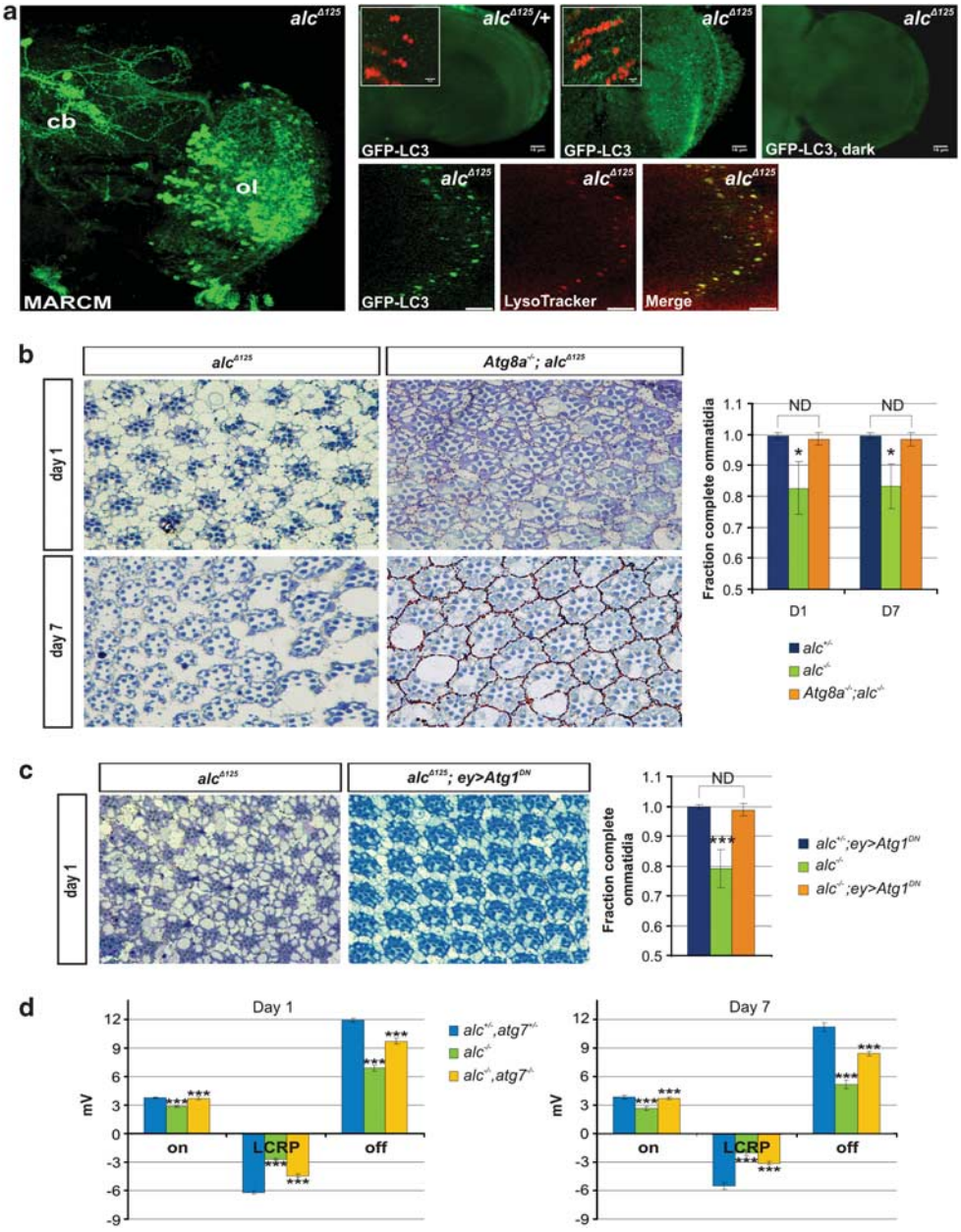

background. Interestingly, a number of other studies suggest that autophagy may be detrimental for cellular survival in particular contexts: activation of autophagy in flies expressing human amyloid beta peptide ($A\beta_{42}$), a known risk factor for Alzheimer's disease, enhances $A\beta_{42}$-mediated neurodegeneration, while inhibition of autophagy ameliorated the degenerative phenotype.[26] Also, excessive autophagy is lethal in *C. elegans*[27] and overexpression of Atg1 induces apoptotic cell death in *Drosophila*.[11] Furthermore, developmentally induced cell death in the female germline is mediated by autophagy, and obsolete midgut and salivary gland cells are removed by autophagy during metamorphosis. Although complete elimination of salivary glands requires the presence of active caspases, midgut cells solely rely on autophagy for degradation.[9,28,29]

Our results further show that the increased autophagy is accompanied by a rise in TOR activity and likely lack of negative regulatory feedback between autophagy and AMPK. It has been previously shown that prolonged starvation leads to reactivation of TOR, which is necessary for autophagic lysosome reformation.[30] In addition, chronic TOR activity can cause neurodegeneration by producing reactive oxygen species, a process that is normally controlled by sestrins that bind to and activate AMPK.[15] Activation of TOR, however, is not the cause for neurodegeneration in *alc* mutants, as its inhibition further deteriorates *alc* mutant retinas, most likely as a result of further increases in autophagic activity. Interestingly, Löffler *et al*.[31] recently published a study in mammalian cell culture, which shows that ULK1 phosphorylates all three AMPK subunits, leading to a decrease in activating phosphorylation of Thr172 in the α subunit of AMPK and a reduction in its catalytic activity. This is in agreement with our data showing induction of autophagy that leads to a marked decrease of *Drosophila* AMPK Thr184 phosphorylation *in vivo*. Further experiments are needed to unravel the precise molecular nature of this proposed feedback loop. However, collectively, these data clearly suggest the existence of a negative feedback loop, which prevents excessive autophagic induction in conditions of persistent activation.

Therefore, the increased autophagy observed in *alc* mutants is most likely a consequence of several events: increased dS6K activity, the presence of AMPK-independent, possibly also TOR-independent mechanisms of autophagy induction, as well as the absence of the negative feedback regulation of AMPK. Namely, in energy-deprived conditions, autophagy is predominantly stimulated by AMPK (as compared with other 'default' autophagy inducers), whose activation is attenuated in conditions of persistent autophagy activation via a regulatory feedback loop, in order to prevent excessive autophagic induction. This dominant effect of AMPK on autophagy activation might molecularly be a consequence of AMPK binding to ULK1, even in conditions of lack of AMPK activity, effectively shielding ULK1 from other inducers.[32] In the absence of AMPK, other autophagy inducers could predominantly stimulate the process, while the autophagic machinery would be unable to moderate their effects, resulting in excessive activation. Interestingly, while there is consensus on the fact that AMPK, TOR and ULK1 interact, conflicting data have been reported on the involved ULK1 phosphorylation sites and whether starvation leads to association or dissociation of ULK1 and AMPK.[4,33] As suggested by Shang *et al*.,[33] nutrient deprivation leads to massive dephosphorylation of ULK1 and consequently to dissociation from AMPK and ULK1 activation.

We further observe a phagocytic-like process at the surface of photoreceptor cells and provide evidence that it functions as a compensatory mechanism during metabolic stress. Specifically, morphological data suggest that photoreceptors 'cannibalize' the surrounding cells in early stages of degeneration, a process that can be stimulated (and tissue morphology better preserved) upon enhancement of phagocytic capacity by overexpression of Crq. This is in line with our observation that the ommatidial disarray and photoreceptor loss are secondary to the great enlargement of

Figure 2 Autophagy promotes neurodegeneration in *alc* mutants. (**a**) Left panel: technique for production of eye clones (*eyeless*-driven Flp) results in the appearance of mutant cells also in the brain, as demonstrated by mosaic analysis with a repressible cell marker (MARCM), labeling all *alc* mutant cells in green (GFP). Mutant cells are visible in the central brain (cb) and particularly in the optic lobes (ol). As a result, brain neurodegeneration can be observed in *alc* eye clonal mutants.[13] As the optic lobes contain abundant homozygous *alc* mutant cells, this tissue was used for GFP-LC3 and Lysotracker (co-) localization. Right panels: (parts of) the optic lobe of the brain. *alc* mutant optic lobes display many GFP-LC3-positive punctae, indicating autophagy induction. The staining is substantially decreased in dark-reared flies, suggesting that autophagy is induced following photoreceptor activation and indicating that the GFP-LC3 punctate signal originates from combined energy and AMPK depletion, and not just the absence of AMPK. Scale bars; 15 μm. Insets: magnifications with counterstained nuclei (anti-elav antibody), scale bars; 5 μm. Lower panels: GFP-LC3-positive punctae co-localize with LysoTracker-positive spots (yellow spots on 'Merge' panel), demonstrating the formation of autolysosomes in *alc* mutant flies. Scale bars; 5 μm. See also Supplementary Figure S1 for autophagy induction in *alc* larval fat body. Genotypes: *w,eyFlp; FRT42B,alc$^{\Delta 125}$/FRT42B,tubP-Gal80; tubP-Gal4,UAS-CD8:GFP/+* (MARCM panel), *UAS-GFP-LC3; FRT42D,alc$^{\Delta 125}$/+; EGUF/+* (*alc$^{\Delta 125}$/+* panel) and *UAS-GFP-LC3; FRT42D,alc$^{\Delta 125}$/FRT42D,GMR-hid,l(2)CI-R1; EGUF/+* (*alc$^{\Delta 125}$* panels). (**b**) Downregulation of autophagy significantly rescues retinal degeneration of *alc* mutants. In *Atg8a; alc* double mutants, some vacuolization is still present, however, rhabdomere loss is almost entirely absent, ommatidial organization is preserved and interommatidial space is mostly 'edema' free and comparable to wild-type. Representative *alc$^{\Delta 125}$* controls and rescues are shown for day 1 (top row) and day 7 (bottom row). Genotypes: *yw/Y; FRT42D,alc$^{\Delta 125}$/FRT42D,GMR-hid,l(2)CI-R1; EGUF/+* (*alc$^{\Delta 125}$* control) and *y,Atg8a^{KG07569}/Y; FRT42D,alc$^{\Delta 125}$/FRT42D,GMR-hid,l(2)CI-R1; EGUF/+* (rescue panels). Quantification: heterozygous *alc$^{\Delta 125}$* control (*alc$^{+/-}$*: *yw/Y; FRT42D,alc$^{\Delta 125}$/+; EGUF/+*) is given for comparison (sections not shown). Data are given as the mean fraction of complete ommatidia (containing seven photoreceptors) $\pm$ S.D. *$P<0.05$ for *alc$^{-/-}$* (*alc$^{\Delta 125}$*) compared with rescue. ND, statistically not different. (**c**) *Eyeless*-mediated overexpression of a dominant-negative Atg1 isoform also leads to a significant improvement of retinal morphology (shown for day 1). Genotypes: *alc$^{\Delta 125}$* control and *FRT42D,alc$^{\Delta 125}$/FRT42D,GMR-hid,l(2)CI-R1; EGUF/UAS-Atg1^{K38Q}* (rescue panel). Quantification: heterozygous *alc$^{\Delta 125}$* control (*FRT42D,alc$^{\Delta 125}$/+; EGUF/UAS-Atg1^{K38Q}*) is given for comparison (sections not shown). Data are given as mean values $\pm$ S.D. ***$P<0.001$ for *alc$^{-/-}$* (*alc$^{\Delta 125}$*) compared with rescue. ND, statistically not different. (**d**) ERG recordings taken from 1- and 7-day-old *Atg7$^{-/-}$*; *alc$^{-/-}$* double mutants (orange bars) show significant improvement of 'on-' and 'off-transients' and LCRP when compared with homozygous *alc$^{\Delta 125}$* controls (green bars). The recordings in the rescued flies are partially reverted to wild-type levels, as indicated in comparison with the heterozygous controls (blue bars). Average recording of >15 flies per genotype, 5 recordings per fly, error bars: S.E.M. (***$P<0.001$ in Student's *t*-test, compared with preceding bar). Representative ERG traces are shown in Supplementary Figure S2

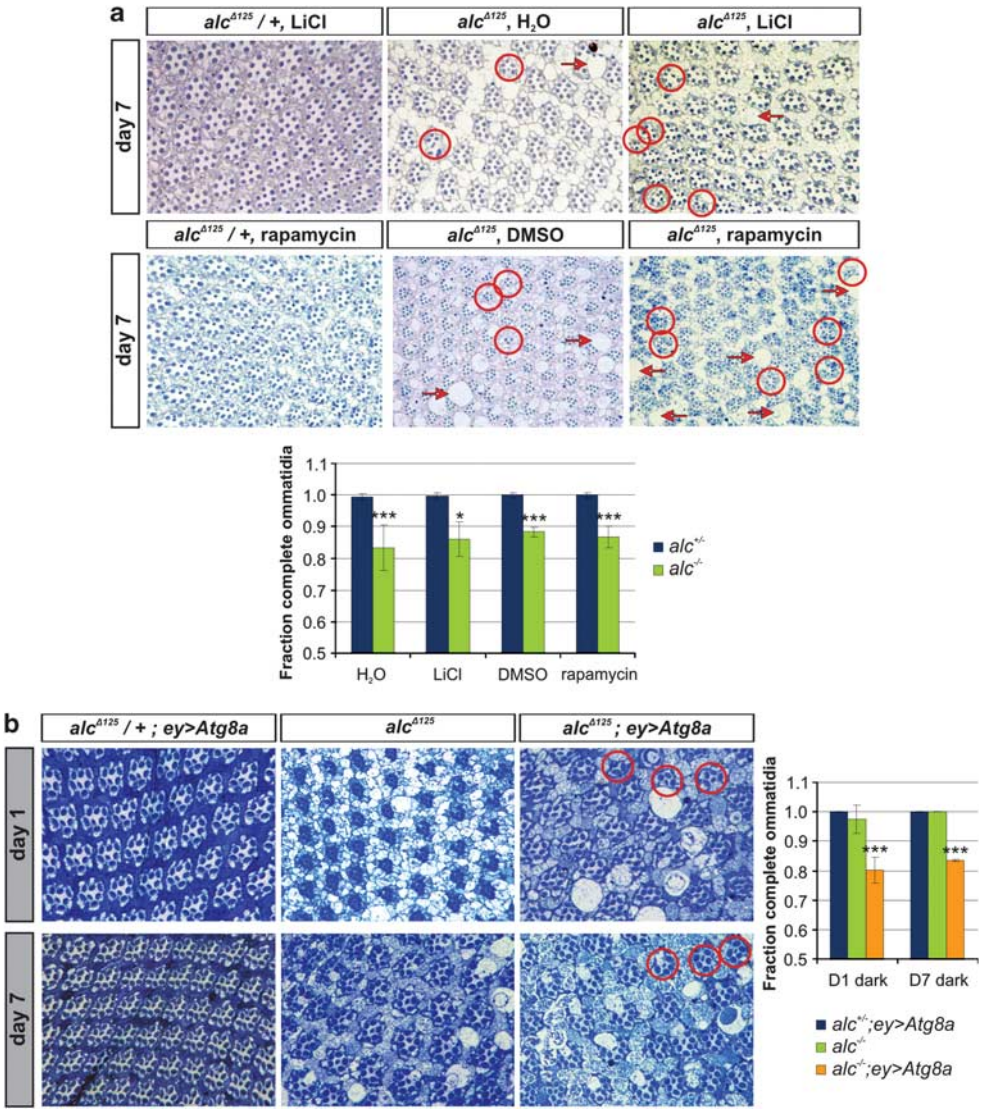

Figure 3 Autophagy is detrimental for cellular survival in *alc* mutant background only. Induction of autophagy using LiCl (top row of panels) and rapamycin (second row of panels) (**a**) and overexpression of the rate-limiting *atg8a* (**b**) in *alc* heterozygous controls (left column) and *alc* mutant retinas (right column). Middle column: *alc* mutant controls; DMSO and water were used as vehicle controls for rapamycin and LiCl, respectively. In heterozygous controls, induction of autophagy does not affect cellular survival. *alc*-induced neurodegeneration is also not rescued by autophagy induction. In contrast, induction of autophagy aggravates cell death in *alc* mutants. This additive effect is clearly revealed after Atg8a overexpression in the dark-reared *alc* mutant flies, a more sensitive background for investigation of additive neurodegenerative effects (while LiCl and rapamycin treatments were performed on light-reared flies). Representative examples of rhabdomere loss and vacuolization are indicated with circles and arrows, respectively. Quantification: $*P<0.05$ and $***P<0.001$ for (**a**) $alc^{-/-}$ ($alc^{\Delta 125}$) compared with $alc^{+/-}$ and (**b**) $alc^{-/-}$ compared with $alc^{-/-}$; *ey>Atg8a*. Data are given as mean values ± S.D. Genotypes: $alc^{\Delta 125}/+$ and $alc^{\Delta 125}$; see Figure 1, *w,Atg8a*^{EP362}*; FRT42D,alc*$^{\Delta 125}$*/+; EGUF/+* (heterozygous control) and *w,Atg8a*^{EP362}*; FRT42D,alc*$^{\Delta 125}$*/ FRT42D,GMR-hid,l(2)CI-R1; EGUF/+*

interommatidial space. In addition, cultured neurons have previously been suggested to harbor phagocytic activities.

Furthermore, in support of this concept, metastatic tumor cells have long been known for their cannibalistic properties, engulfing and ingesting entire live cells, either their siblings or cells from the immune system, thus ensuring their survival or leading to a non-apoptotic form of target cell death termed entosis.[34] Importantly, tumor cells may use this peculiar function also to feed in conditions of low nutrient supply.[35,36] Moreover, it has been suggested that cell cannibalism itself requires a relatively normal energy supply from aerobic respiration, as it directly correlates with residual mitochondrial function.[18] This would explain why the phagocytic-like process is seen in early stages of degeneration in *alc* mutants, while the photoreceptors are still rich in cellular content. Notwithstanding the differences between tumor cell cannibalism and the process observed in our study (which involves engulfment of large vesicles, but not entire cells and, judging by vesicle morphology, appears to be somewhat more discriminative for content), the essence of these pathologies seems similar.

Interestingly, the autophagic and the phagocytic pathways are functionally interconnected, as demonstrated in

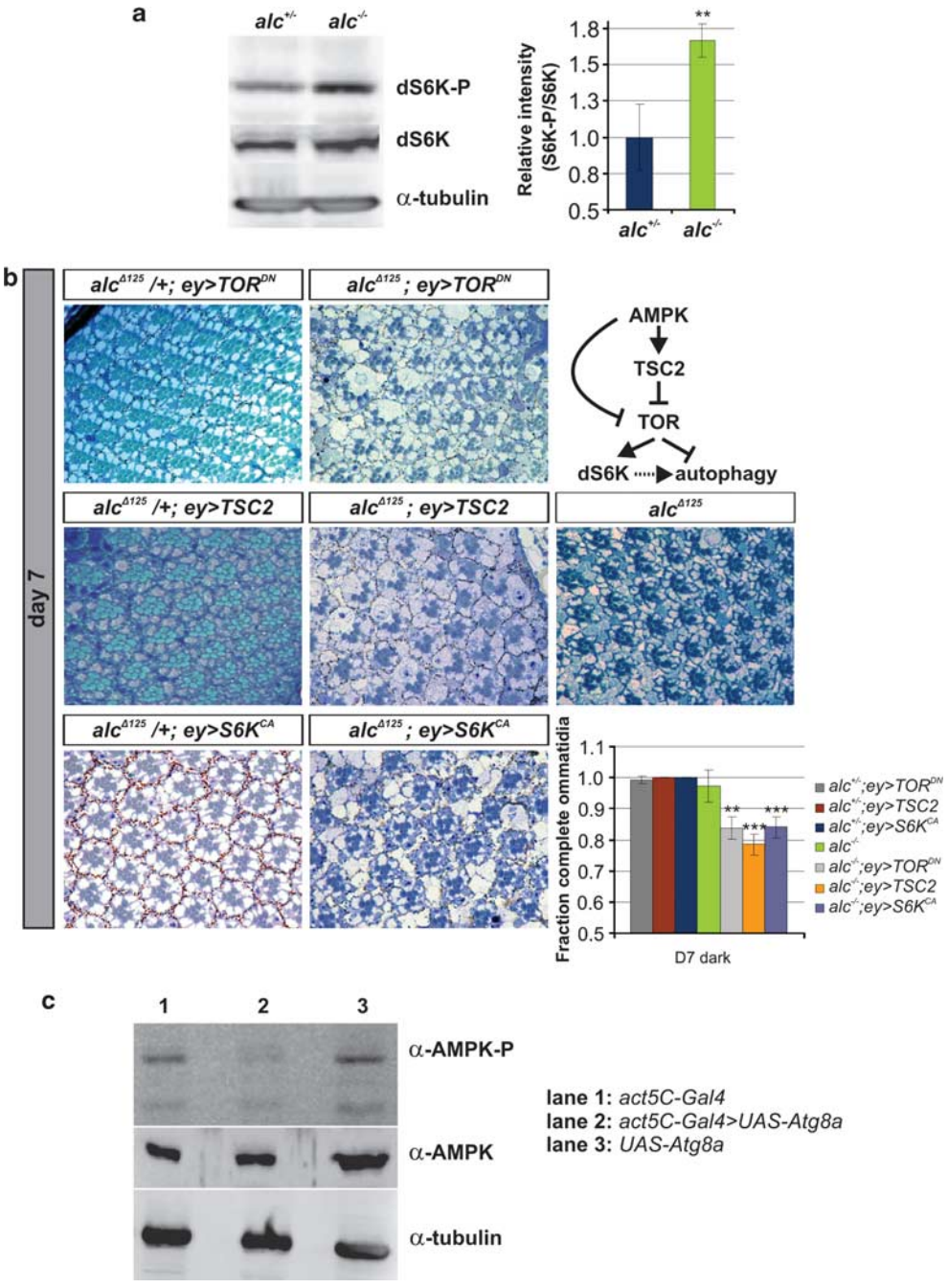

Figure 4 Increased TOR activity and the lack of negative regulatory feedback between autophagy and AMPK in *alc* mutants. (**a**) TOR activity is stimulated in *alc* mutants, as evidenced by increased phosphorylation of its downstream target S6 kinase (dS6K).[15] Depicted is a representative immunoblot of head extracts (~ 100 of each genotype) from heterozygous control (left) and *alc* mutant flies (right), using an antibody specific for phosphorylated dS6K. The bar graph depicts quantification of the increased phosphorylation corrected for levels of non-phosphorylated dS6K and normalized to control values. Represented are mean values ($n = 6$) ± S.D., $^{**}P < 0.01$ in Student's *t*-test. Genotypes as in Figure 1. (**b**) Downregulation of TOR using a dominant-negative allele (TOR^{DN}, top row) or TSC2 overexpression (middle row) results in aggravation of the neurodegenerative phenotype at day 1 (not shown) and day 7 (shown here). Expression of a constitutively active dS6K ($S6K^{CA}$) also exacerbates *alc*-mediated neurodegeneration. Flies were reared in the dark so as to sensitize the background for investigation of additive effects (see comment to Figure 3). Quantification: $^{**}P < 0.01$, $^{***}P < 0.001$ when compared with $alc^{-/-}$ ($alc^{\Delta 125}$). Data are given as mean values ± S.D. Genotypes: *FRT42D,*$alc^{\Delta 125}$*/+ ; EGUF/UAS-TOR*^{FRB} and *FRT42D,*$alc^{\Delta 125}$*/+ ; EGUF/UAS-TSC2* and *FRT42D,*$alc^{\Delta 125}$*/+ ; EGUF/UAS-S6K*^{STDE}plus corresponding homozygous *alc* mutants. $alc^{\Delta 125}$ as in Figure 1. (**c**) Increased autophagy reduces activating phosphorylation of α-AMPK, suggesting a negative regulatory feedback loop. Shown is a representative immunoblot from control lines (*act5C-Gal4* driver line (lane 1) and $atg8a^{EP}$ line (lane 3)) and flies in which autophagy was induced by ubiquitous overexpression of *atg8a* (lane 2). All flies originated from the same cross. Genotypes: *yw/Y; act5C-Gal4/+* and $Atg8a^{EP}$*/yw; act5C-Gal4/+* and $Atg8a^{EP}$*/yw*

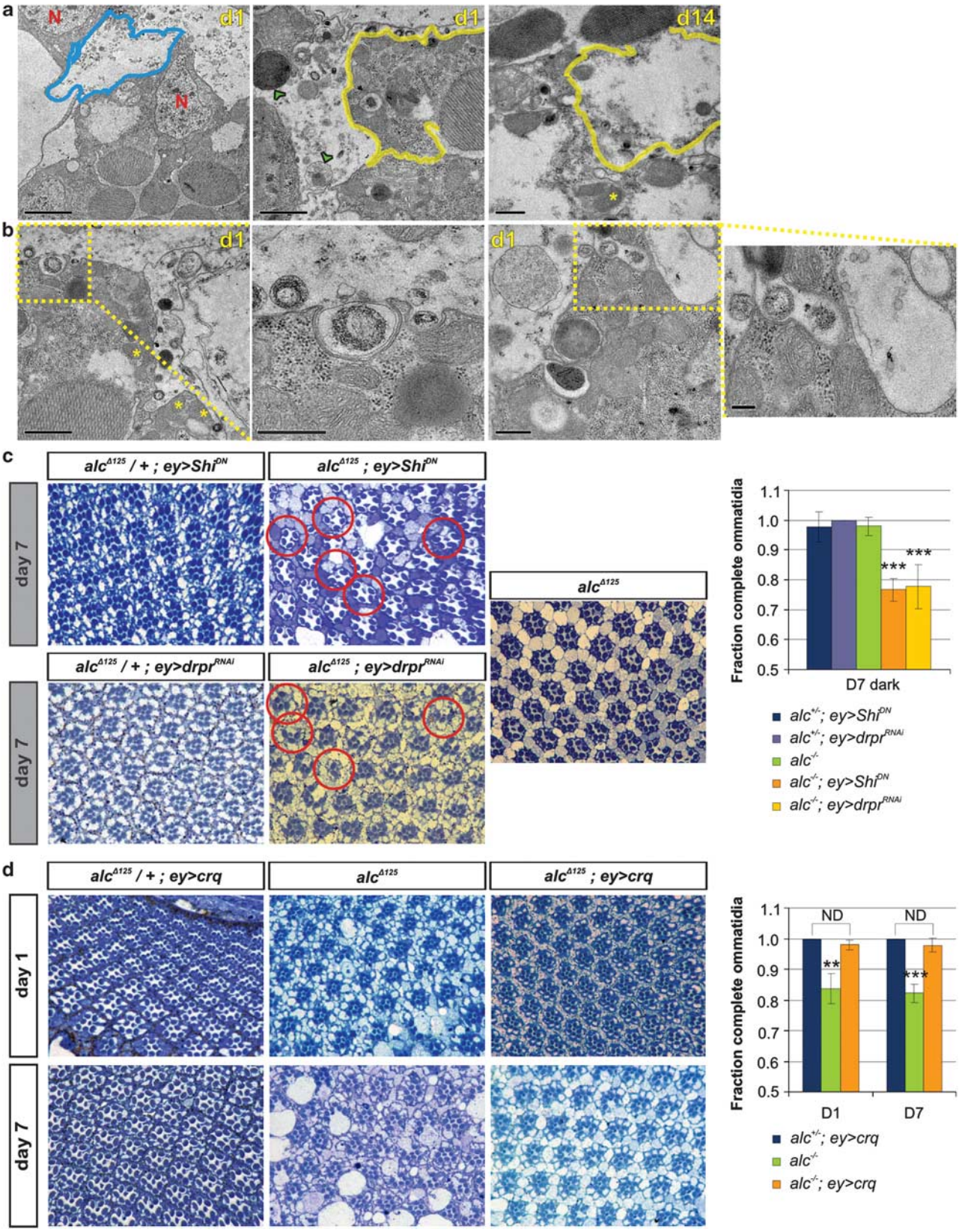
a
N
d1
N
d1
d14
b
d1
d1
c
alc^Δ125 / + ; ey>Shi^DN
alc^Δ125 ; ey>Shi^DN
day 7
alc^Δ125
alc^Δ125 / + ; ey>drpr^RNAi
alc^Δ125 ; ey>drpr^RNAi
day 7
Fraction complete ommatidia
1.1
1.0
0.9
0.8
0.7
0.6
0.5
***
***
D7 dark
alc^+/-; ey>Shi^DN
alc^+/-; ey>drpr^RNAi
alc^-/-
alc^-/-; ey>Shi^DN
alc^-/-; ey>drpr^RNAi
d
alc^Δ125 / + ; ey>crq
alc^Δ125
alc^Δ125 ; ey>crq
day 1
day 7
Fraction complete ommatidia
1.1
1.0
0.9
0.8
0.7
0.6
0.5
ND
ND
**
***
D1
D7
alc^+/-; ey>crq
alc^-/-
alc^-/-; ey>crq

macrophages, where LC3 is recruited to apoptotic cell phagosomes and proteins involved in autophagy enhance phagosome maturation.[37,38] Similarly, activation of Toll-like receptor facilitates phagosome maturation and at the same time engages autophagy.[39] In addition, autophagy induces apoptotic cells to present a signal to ensure their clearance by phagocytes, which is crucial for mouse embryonic morphogenesis.[40] It would therefore be reasonable to assume that the occurrence of both of these processes in *alc* mutant tissues could be a consequence of mutual activation.

In conclusion, we here provide new evidence for roles of autophagy and phagocytosis in the cellular response to metabolic stress and in cell death (Figure 6). These novel mechanisms by which cells respond to conditions of extreme metabolic perturbation open new avenues for research that will contribute to a better understanding of human health and disease.

Materials and Methods

***Drosophila* strains and culture conditions.** A β-AMPK null allele (imprecise *P*-element excision, $alc^{\Delta 125}$) recombined to *FRT{ry*$^{+\,t7.2}$*= neoFRT} 42D* was used for the production of genetic clones.[13] Eye clonal mutants were produced using *eyeless-Gal4,UAS-Flp (EGUF); GMR-hid*. For MARCM analysis, we used flies of the following genotype: *w,eyFlp; FRT42B,alc*$^{\Delta 125}$*/Cyo* and *w; FRT42B,tubP-Gal80/CyO; tubP-Gal4, UAS-CD8:GFP*.

Lines carrying *UAS-DIAP1*, *Atg8a*^{EP362}, *Atg8a*^{KG07569}, *UAS-dS6K*^{STDE} and *UAS-Shi*^{K44A} were obtained from the Bloomington Stock Center (Bloomington, IN, USA). *Atg7*^{d4}, *UAS-dTOR*^{FRB}, *UAS-Atg1*^{K38Q}, *UAS-TSC2*, *UAS-GFP-LC3* and *UAS-crq* lines were kind gifts from T Neufeld (University of Minnesota, Minneapolis, MN, USA), D Pan (Johns Hopkins University School of Medicine, Baltimore, MD, USA), H Stenmark (Institute for Cancer Research, Oslo, Norway) and N Franc (The Scripps Research Institute, La Jolla, CA, USA). *Atg7*^{d4} was recombined to *FRT42D,alc*$^{\Delta 125}$ for the production of genetic clones. *drpr*^{GD2628} and *drpr*^{GD14423} were obtained from the VDRC (Vienna, Austria). Overexpression (*UAS*-) constructs were driven by *eyeless-Gal4*.

Flies were reared under controlled temperature conditions of 25 °C and, when specified, under 12-h light/dark cycle or in constant darkness from embryonic stage onward. For drug treatments, flies were kept on instant medium (Formula 4-24 Blue, Carolina Biological Supply Company, Burlington, NC, USA) supplemented either with 2 μM rapamycin (Sigma-Aldrich, Bornem, Belgium) or 5 mM LiCl (Merck, Overijse, Belgium). DMSO and water were used as vehicle controls, respectively. For other experiments, flies were kept on the standard fly medium. For larval starvation experiments, early third instar larvae were put on a 20% sucrose solution for 4 h.[16] Fat body clones were induced with heat shock (hs)*-Flp* (2 h hs at 37 °C of 0 to 8-h-old embryos).

Tissue sections, histological staining and quantification of photoreceptor loss. For semi-thin plastic sections of the retina, aged flies were dissected and fixed in 2% glutaraldehyde, 1% OsO_4, 50 mM sodium cacodylate and 4.2 mM HCl for 30 min on ice and postfixed in 2% OsO_4, 50 mM sodium cacodylate for 2 h on ice. Subsequently, fly heads were dehydrated through acetone series and embedded with the Spurr Low Viscosity Embedding kit (Polysciences, Eppelheim, Germany). The 1-μm sections were stained with 1% Toluidine Blue in 2% disodiumtetraborate. Images were obtained using an FV1000 microscope (Olympus, Aartselaar, Belgium) and Cell^D imaging software (Olympus). For quantification, the fraction of ommatidia that contained seven photoreceptors was calculated (number of 'complete' ommatidia/total number of ommatidia) using identical magnifications of two different eye sections from at least five flies ($\geq$10 sections per genotype, $\geq \pm$300 ommatidia). Data are expressed as mean fraction $\pm$ S.D. *P*-values were calculated using Student's *t*-test. Although 7-day-old *alc* flies exhibited the same fraction of photoreceptor loss as 1-day-old mutants, the progressive nature of neurodegeneration was evidenced by increased vacuolization as well as enhanced photoreceptor loss in 14- and 34-day-old *alc* flies.[13]

Transmission electron microscopy. For ultrathin sections of the retina, flies were decapitated and heads were fixed overnight in Karnovsky fixative

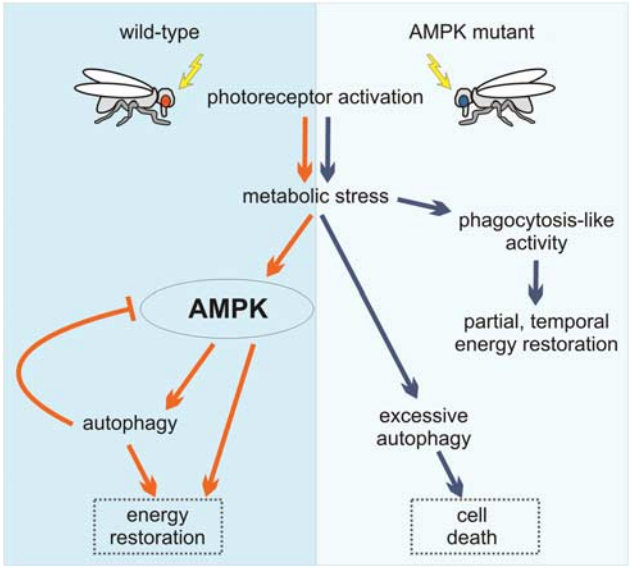

Figure 6 An overview of events following metabolic stress in wild-type and AMPK mutant photoreceptors. Left panel: activation of wild-type photoreceptors leads to metabolic stress, followed by increased AMPK and autophagic activity that together restore energy levels. Autophagy is controlled by negative feedback regulation to AMPK. Right panel: AMPK mutant photoreceptors respond to metabolic perturbation by inducing phagocytic activity and autophagy, in an AMPK-independent way. The suggested lack of AMPK-mediated feedback leads to excessive autophagy and eventually to cell death

Figure 5 Neuronal survival in early stages of degeneration is dependent on phagocytosis-like cell cannibalism in *alc* mutants. (**a**) In early stages of neurodegeneration (day 1), pigment cells (outlined blue, left panel) appear to mostly contain degraded cellular material, in contrast to neighboring photoreceptors (outlined yellow, middle panel), which are rich in cellular content. Multiple vesicular structures are observed in the pigment cells (examples marked with green arrowheads), some of which appear to be engulfed by surrounding photoreceptors. Photoreceptors cells (outlined yellow, right panel) also have reduced cellular contents by day 14. Scale bars: 2 μm (panel on far left) and 1 μm (middle and right panel). (**b**) Details of engulfment of material by photoreceptors at day 1. Panels 2 and 4 represent enlargements of boxed areas. Scale bars: 1 μm (panel on far left), 500 nm (panels 2 and 3) and 200 nm (panel on far right). Representative nuclei and mitochondria are indicated with red N and a yellow asterisk, respectively. (**c**) Expression of a *shibire* dominant-negative allele (Shi^{DN}) or downregulation of Draper ($drpr^{RNAi}$) aggravates *alc*-mediated neurodegeneration (compare right $alc^{\Delta 125}$ panel to middle panels). Flies were reared in the dark so as to sensitize the background for investigation of additive effects (see comment to Figure 3). Representative examples of rhabdomere loss are indicated with circles. Quantification: ***$P<0.001$ for $alc^{-/-}$; *ey*$>$ Shi^{DN} and $alc^{-/-}$; *ey*$>$ $drpr^{RNAi}$ compared with $alc^{-/-}$ ($alc^{\Delta 125}$). Data are given as mean values $\pm$ S.D. Genotypes: $alc^{\Delta 125}$ control as in Figure 1, *FRT42D,alc*$^{\Delta 125}$*/+; EGUF/UAS-Shi*^{K44A} and *FRT42D,alc*$^{\Delta 125}$*/+; EGUF/UAS-drpr*^{RNAi} (heterozygous controls), *FRT42D,alc*$^{\Delta 125}$*/FRT42D,GMR-hid,l(2)CI-R1; EGUF/UAS-Shi*^{K44A} and *FRT42D,alc*$^{\Delta 125}$*/FRT42D,GMR-hid,l(2)CI-R1; EGUF/UAS- drpr*^{RNAi}. (**d**) Overexpression of the engulfment receptor Crq rescues neurodegeneration of *alc* mutants (compare right column to middle column). Quantification: **$P<0.01$, ***$P<0.001$ for $alc^{-/-}$ ($alc^{\Delta 125}$) compared with $alc^{-/-}$; *ey*$>$ *crq*. ND, statistically not different. Data are given as mean values $\pm$ S.D. Genotypes: $alc^{\Delta 125}$ control as in Figure 1, *FRT42D,alc*$^{\Delta 125}$*/+; EGUF/UAS-crq* (heterozygous control) and *FRT42D,alc*$^{\Delta 125}$*/FRT42D,GMR-hid,l(2)CI-R1; EGUF/UAS-crq*

(2% paraformaldehyde, 2% glutaraldehyde in 50 mM sodium cacodylate and 4.2 mM HCl). Subsequently, the samples were postfixed in 2% OsO_4 for 2 h on ice, dehydrated in ethanol series and stained with 4% uranyl-acetate for 30 min in the dark. The embedding resin, Agar100 (Agar Scientific Ltd, Stansted, UK), was introduced in a mixture with decreasing concentration of propylene oxide, during a period of ~20 h. Ultrathin (70 nm) sections were poststained with 4% uranyl-acetate and lead citrate. Images were obtained using a transmission electron microscope JEM-2100 (JEOL, Zaventem, Belgium) at the KU Leuven Electron Microscopy Core Facility.

GFP-LC3 and LysoTracker staining. For GFP-LC3 detection, brains of 1-day-old adult flies were dissected in ice-cold phosphate-buffered saline (PBS) and fixed in 4% formaldehyde. Samples were then incubated overnight with anti-GFP antibody (1 : 500, A6455, Invitrogen, Gent, Belgium) in PAXD (1 × PBS, 5% BSA, 0.3% Triton X-100 and 0.3% sodium deoxycholate), 2 h with cyanine 3-conjugated secondary antibody (Jackson ImmunoResearch, Newmarket, UK) and mounted in Vectashield mounting medium (Vector Laboratories, Brussels, Belgium). Nuclei were counterstained with anti-elav antibody (1 : 200, 7E8A10, DSHB, Iowa City, IA, USA).

For LysoTracker staining, fat bodies from fed or starved third instar larvae, or adult brains were dissected in PBS and incubated for 5 min in 1 μM LysoTracker Red DND-99 (Invitrogen). Subsequently, samples were washed for 5 min in PBS and transferred onto glass slides, covered and immediately photographed live on an Olympus FV1000 confocal microscope. Simultaneous detection of the LysoTracker and GFP-LC3 signal in adult brains was performed as described for LysoTracker staining, using the endogenous fluorescent signal from GFP-LC3.

Western blotting. A total of 100 heads from each fly strain were collected and homogenized in cell lysis buffer (50 mM Tris-HCl (pH 7.5), 150 mM NaCl, 1 mM EDTA, 0.1% SDS, 0.5% deoxycholic acid, 1% Igepal CA-630 and protease and phosphatase inhibitor cocktail tablets (Roche, Vilvoorde, Belgium)). Lysates were cleared by centrifugation, boiled in 1X SDS sample buffer, resolved by SDS-PAGE, transferred onto nitrocellulose membranes and probed with anti-phospho-*Drosophila*-S6K (Thr398; 1 : 1000, #9209, Cell Signaling, Leiden, The Netherlands), anti-S6K-α (1 : 200, sc-230, Santa Cruz Biotechnology, Heidelberg, Germany), anti-phospho-AMPK-α (Thr172; 1 : 2000, #4188, Cell signaling), anti-AMPK-α 1/2 (1 : 500, ab80039, Abcam, Cambridge, UK) and with anti-α-tubulin (1 : 2500, ab4074, Abcam), and subsequently with peroxidase-conjugated secondary antibody (1 : 10 000; Jackson ImmunoResearch). Chemiluminescence was detected using a LAS-3000 Imager system (Fuji Film, Wavre, Belgium). Quantification was performed using the AIDA image analysis software (Raytest, Tilburg, The Netherlands).

ERG measurements. For ERG recordings, flies were fixed onto glass slides with glue. A reference electrode was inserted in the thorax, and the recording electrode, filled with 3 M NaCl, was placed on the eye surface. Light flashes of 1 s were delivered using a halogen lamp. Data were digitized with pClamp (Molecular Devices, Sunnyvale, CA, USA) and analyzed with Clampfit software (Molecular Devices).

Conflict of Interest

The authors declare no conflict of interest.

Acknowledgements. We thank P Agostinis (KU Leuven) for scientific discussion, the P Verstreken lab (KU Leuven) for help with ERG measurements, P Baatsen from the Electron Microscopy Core Facility (VIB – KU Leuven) for help with electron microscopy, I Pintens and W Robyns for technical assistance and the Bloomington and VDRC Stock Centers for reagents. MG and JM are supported by IWT. JP is supported by a postdoctoral grant from FWO.

1. He C, Klionsky DJ. Regulation mechanisms and signaling pathways of autophagy. *Annu Rev Genet* 2009; **43**: 67–93.
2. Hardie DG. AMP-activated protein kinase: an energy sensor that regulates all aspects of cell function. *Genes Dev* 2011; **25**: 1895–1908.
3. Egan DF, Shackelford DB, Mihaylova MM, Gelino S, Kohnz RA, Mair W *et al.* Phosphorylation of ULK1 (hATG1) by AMP-activated protein kinase connects energy sensing to mitophagy. *Science* 2011; **331**: 456–461.
4. Kim J, Kundu M, Viollet B, Guan KL. AMPK and mTOR regulate autophagy through direct phosphorylation of Ulk1. *Nat Cell Biol* 2011; **13**: 132–141.
5. Lipinski MM, Hoffman G, Ng A, Zhou W, Py BF, Hsu E *et al.* A genome-wide siRNA screen reveals multiple mTORC1 independent signaling pathways regulating autophagy under normal nutritional conditions. *Dev Cell* 2010; **18**: 1041–1052.
6. Shen HM, Codogno P. Autophagic cell death: Loch Ness monster or endangered species? *Autophagy* 2011; **7**: 457–465.
7. Denton D, Nicolson S, Kumar S. Cell death by autophagy: facts and apparent artefacts. *Cell Death Differ* 2011; **19**: 87–95.
8. Berry DL, Baehrecke EH. Growth arrest and autophagy are required for salivary gland cell degradation in *Drosophila*. *Cell* 2007; **131**: 1137–1148.
9. Denton D, Shravage B, Simin R, Mills K, Berry DL, Baehrecke EH *et al.* Autophagy, not apoptosis, is essential for midgut cell death in *Drosophila*. *Curr Biol* 2009; **19**: 1741–1746.
10. McPhee CK, Logan MA, Freeman MR, Baehrecke EH. Activation of autophagy during cell death requires the engulfment receptor Draper. *Nature* 2010; **465**: 1093–1096.
11. Scott RC, Juhasz G, Neufeld TP. Direct induction of autophagy by Atg1 inhibits cell growth and induces apoptotic cell death. *Curr Biol* 2007; **17**: 1–11.
12. Kroemer G, Galluzzi L, Vandenabeele P, Abrams J, Alnemri ES, Baehrecke EH *et al.* Classification of cell death: recommendations of the nomenclature committee on cell death 2009. *Cell Death Differ* 2009; **16**: 3–11.
13. Spasić MR, Callaerts P, Norga KK. *Drosophila* alicorn is a neuronal maintenance factor protecting against activity-induced retinal degeneration. *J Neurosci* 2008; **28**: 6419–6429.
14. Rusten TE, Lindmo K, Juhasz G, Sass M, Seglen PO, Brech A *et al.* Programmed autophagy in the *Drosophila* fat body is induced by ecdysone through regulation of the PI3K pathway. *Dev Cell* 2004; **7**: 179–192.
15. Lee JH, Budanov AV, Park EJ, Birse R, Kim TE, Perkins GA *et al.* Sestrin as a feedback inhibitor of TOR that prevents age-related pathologies. *Science* 2010; **327**: 1223–1228.
16. Scott RC, Schuldiner O, Neufeld TP. Role and regulation of starvation-induced autophagy in the *Drosophila* fat body. *Dev Cell* 2004; **7**: 167–178.
17. Doherty GJ, McMahon HT. Mechanisms of endocytosis. *Annu Rev Biochem* 2009; **78**: 857–902.
18. Malorni W, Matarrese P, Tinari A, Farrace MG, Piacentini M. Xeno-cannibalism: a survival 'escamotage'. *Autophagy* 2007; **3**: 75–77.
19. Kinchen JM, Doukoumetzidis K, Almendinger J, Stergiou L, Tosello-Trampont A Sifri CD *et al.* A pathway for phagosome maturation during engulfment of apoptotic cells. *Nat Cell Biol* 2008; **10**: 556–566.
20. Freeman MR, Delrow J, Kim J, Johnson E, Doe CQ. Unwrapping glial biology: Gcm target genes regulating glial development, diversification, and function. *Neuron* 2003; **38**: 567–580.
21. Franc NC, Heitzler P, Ezekowitz RA, White K. Requirement for croquemort in phagocytosis of apoptotic cells in *Drosophila*. *Science* 1999; **284**: 1991–1994.
22. Venkatachalam K, Long AA, Elsaesser R, Nikolaeva D, Broadie K, Montell C. Motor deficit in a *Drosophila* model of mucolipidosis type IV due to defective clearance of apoptotic cells. *Cell* 2008; **135**: 838–851.
23. Wang RC, Levine B. Autophagy in cellular growth control. *FEBS Lett* 2010; **584**: 1417–1426.
24. Yen WL, Klionsky DJ. How to live long and prosper: autophagy, mitochondria, and aging. *Physiology* 2008; **23**: 248–262.
25. Tschäpe JA, Hammerschmied C, Muhlig-Versen M, Athenstaedt K, Daum G, Kretzschmar D. The neurodegeneration mutant löchrig interferes with cholesterol homeostasis and Appl processing. *EMBO J* 2002; **21**: 6367–6376.
26. Ling D, Song HJ, Garza D, Neufeld TP, Salvaterra PM. Abeta42-induced neurodegeneration via an age-dependent autophagic-lysosomal injury in *Drosophila*. *PLoS One* 2009; **4**: e4201.
27. Kang C, You YJ, Avery L. Dual roles of autophagy in the survival of *Caenorhabditis elegans* during starvation. *Genes Dev* 2007; **21**: 2161–2171.
28. Martin DN, Baehrecke EH. Caspases function in autophagic programmed cell death in *Drosophila*. *Development* 2004; **131**: 275–284.
29. Nezis IP, Lamark T, Velentzas AD, Rusten TE, Bjorkoy G, Johansen T *et al.* Cell death during *Drosophila melanogaster* early oogenesis is mediated through autophagy. *Autophagy* 2009; **5**: 298–302.
30. Yu L, McPhee CK, Zheng L, Mardones GA, Rong Y, Peng J *et al.* Termination of autophagy and reformation of lysosomes regulated by mTOR. *Nature* 2010; **465**: 942–946.
31. Löffler AS, Alers S, Dieterle AM, Keppeler H, Franz-Wachtel M, Kundu M *et al.* Ulk1-mediated phosphorylation of AMPK constitutes a negative regulatory feedback loop. *Autophagy* 2011; **7**: 696–706.
32. Behrends C, Sowa ME, Gygi SP, Harper JW. Network organization of the human autophagy system. *Nature* 2010; **466**: 68–76.
33. Shang L, Chen S, Du F, Li S, Zhao L, Wang X. Nutrient starvation elicits an acute autophagic response mediated by Ulk1 dephosphorylation and its subsequent dissociation from AMPK. *Proc Natl Acad Sci USA* 2011; **108**: 4788–4793.
34. Matarrese P, Ciarlo L, Tinari A, Piacentini M, Malorni W. Xeno-cannibalism as an exacerbation of self-cannibalism: a possible fruitful survival strategy for cancer cells. *Curr Pharm Des* 2008; **14**: 245–252.
35. Fais S. Cannibalism: a way to feed on metastatic tumors. *Cancer Lett* 2007; **258**: 155–164.

36. Lugini L, Matarrese P, Tinari A, Lozupone F, Federici C, Iessi E *et al.* Cannibalism of live lymphocytes by human metastatic but not primary melanoma cells. *Cancer Res* 2006; **66**: 3629–3638.
37. Florey O, Kim SE, Sandoval CP, Haynes CM, Overholtzer M. Autophagy machinery mediates macroendocytic processing and entotic cell death by targeting single membranes. *Nat Cell Biol* 2011; **13**: 1335–1343.
38. Shui W, Sheu L, Liu J, Smart B, Petzold CJ, Hsieh TY *et al.* Membrane proteomics of phagosomes suggests a connection to autophagy. *Proc Natl Acad Sci USA* 2008; **105**: 16952–16957.
39. Sanjuan MA, Dillon CP, Tait SW, Moshiach S, Dorsey F, Connell S *et al.* Toll-like receptor signalling in macrophages links the autophagy pathway to phagocytosis. *Nature* 2007; **450**: 1253–1257.
40. Qu X, Zou Z, Sun Q, Luby-Phelps K, Cheng P, Hogan RN *et al.* Autophagy gene-dependent clearance of apoptotic cells during embryonic development. *Cell* 2007; **128**: 931–946.
41. Wang T, Montell C. Phototransduction and retinal degeneration in *Drosophila*. *Pflugers Arch* 2007; **454**: 821–847.

Supplementary Information accompanies the paper on Cell Death and Differentiation website (http://www.nature.com/cdd)